Journal of Materials Chemistry

Cite this: J. Mater. Chem., 2011, 21, 9326

www.rsc.org/materials

PAPER

Highly efficient solution-processed green and red electrophosphorescent devices enabled by small-molecule bipolar host material†

Minrong Zhu,[a] Tengling Ye,[b] Xun He,[a] Xiaosong Cao,[a] Cheng Zhong,[a] Dongge Ma,*[b] Jingui Qin[a] and Chuluo Yang*[a]

Received 7th March 2011, Accepted 7th April 2011
DOI: 10.1039/c1jm10987a

A solution-processable host molecule **TPO** comprised of hole-transporting triphenylamine and electron-transporting oxadiazole has been synthesized. Through *meta*-linkage between the donor and the acceptor, complete charge localization of the HOMO and LUMO and proper triplet energy are imparted. The new compound shows good thermal stability with a high glass-transition temperature of 131 °C. Smooth and homogeneous film can be obtained by spin-coating from a **TPO**/iridium complex blend as probed by atomic force microscopy. The solution-processed red phosphorescent organic light-emitting device (PhOLED) achieves a maximum current efficiency of 13.3 cd A^{-1} with Commission Internationale de l'Eclairage coordinates of (0.64, 0.36); while the green device reaches a maximum current efficiency of 40.8 cd A^{-1}, and the value is still as high as 39.6 cd A^{-1} at a practical luminance of 1000 cd m^{-2}. The low roll-off can be attributed to the bipolar nature of the host material **TPO**. An optimized device further elevates the efficiency to 56.8 cd A^{-1}, which is among the highest ever reported for small-molecule based green PhOLEDs fabricated by a wet process.

Introduction

In the past decade, considerable efforts have been focused on phosphorescent organic light emitting diodes (PhOLEDs) to upgrade the efficiency of OLEDs since the phosphorescent dyes of heavy metal complexes can harvest both singlet and triplet excitons to achieve the internal quantum efficiency of devices up to 100% theoretically.[1] Until now, most of the efficient PhOLEDs have been fabricated through vacuum thermal evaporation in multilayer configurations.[2,3] But the layer-by-layer deposition technique allowing for complicated device structures to achieve high performance is a rather costly process. Meanwhile, pixelation using evaporation masks limits large-size scalabilities and high-resolution applications. It is generally believed that solution-based processes, such as spin-coating or ink-jet printing, are relatively inexpensive and can be utilized for the preparation of large-area displays.[4–6] Though numerous efforts have been carried out to improve the performance of solution-processed PhOLEDs, their efficiencies are still far behind the vacuum-evaporated devices.[7–9] To date, solution-processed PhOLEDs are mainly focused on polymeric materials by incorporation of heavy metal complexes through physical blending in polymer hosts like poly(9-vinylcarbazole) (PVK)[10–15] or chemical bonding on polymer chains.[16–19] Unfortunately, the applicability of polymeric materials are greatly hampered by intrinsic disadvantages, such as the uncertain molecular structure and difficulty in purification, while the purity of materials has a great influence on electroluminescence performance. In contrast, small molecules have exact molecular structure and can be easily purified to overcome the shortcomings of polymeric PhOLEDs.[20,21] Therefore it is of important significance to develop highly efficient small-molecule based PhOLEDs by solution-processing.[22,23]

Due to the relatively long excited state lifetimes of triplet emitters, the heavy metal complexes are usually doped into host materials to reduce the self-quenching and triplet–triplet annihilation. By the combination of both hole and electron transporting moieties in one molecule, bipolar molecules in the quest for highly efficient PhOLEDs have aroused considerable interest because they enable a balanced density of charge and simplify device structures. Compared with vacuum-deposited counterparts,[24–26] small-molecule based bipolar hosts for solution-processable PhOLEDs have rarely been reported.[27–30] Kakimoto *et al.* reported solution-processed green PhOLEDs hosted by bipolar triphenylamine/benzimidazole hybrids, and a maximum current efficiency of 27.3 cd A^{-1} was realized by using *fac*-tris(2-phenylpyridine)iridium ($Ir(ppy)_3$) as guest.[27,28] In our previous work, yellow- and red-emitting phosphorescent organic light emitting devices from a small molecule bipolar host and iridium complexes were fabricated by a wet process.[29] A maximum

[a]*Department of Chemistry, Hubei Key Lab on Organic and Polymeric Optoelectronic Materials, Wuhan University, Wuhan, 430072, People's Republic of China. E-mail: clyang@whu.edu.cn*
[b]*State Key Laboratory of Polymer Physics and Chemistry, Changchun Institute of Applied Chemistry, Chinese Academy of Sciences, Changchun, 130022, People's Republic of China. E-mail: mdg1014@ciac.jl.cn*

† Electronic supplementary information (ESI) available: External quantum efficiency *versus* current density curves for devices. See DOI: 10.1039/c1jm10987a

current efficiency of 20.0 cd A^{-1} for a yellow-emitting OLED, and 4.6 cd A^{-1} for a red-emitting OLED were achieved under ambient conditions. However, the large energy barrier between the anode and emission layer caused high turn-on voltages in the range of 7.0–15.1 V.

Herein, we designed and synthesized a new oxadiazole/triphenylamine hybrid (**TPO**) aiming to act as host material for solution-processable PhOLEDs. The oxadiazole unit was introduced as an electron-accepting component due to its good electron mobility. Triphenylamine (TPA) has a high triplet energy (3.04 eV) and good hole-transporting ability as well as a high-lying highest occupied molecular orbital (HOMO) level. Through *meta*-linkage of the electron-rich triphenylamine moieties and electron-deficient oxadiazole unit, complete separation of the HOMO and lowest occupied molecular orbital (LUMO) at the hole- and electron-transporting moieties was implemented. Furthermore the *meta*-linkage could alleviate the intramolecular charge transfer from the donor to the acceptor, and thus proper triplet energy was maintained to make them capable of hosting green and red phosphorescent emitters. Additionally, the hybrid shows a close HOMO level (5.19 eV) to the work function of the common anode buffer layer poly(ethylenedioxythiophene):poly(styrenesulfonate) (PEDOT:PSS) (5.2 eV), and thus allows efficient hole injection. When using Ir $(ppy)_3$ or bis(2,4-diphenylquinolyl-N,$C^{2'}$)iridium(acetylacetonate) [$(PPQ)_2$Ir(acac)] as guest, highly efficient green and red PhOLEDs were realized by solution-processing, with maximum current efficiencies of 56.8 cd A^{-1} and 13.3 cd A^{-1}, respectively, which are among the highest ever reported for small-molecule based PhOLEDs fabricated by a wet process.

Experimental section

General information

^{1}H NMR and ^{13}C NMR spectra were measured on a MECUYR-VX300 spectrometer. Elemental analyses of carbon, hydrogen, and nitrogen were performed on a Vario EL III microanalyzer. Mass spectra were measured on a ZAB 3F-HF mass spectrophotometer. UV–vis absorption spectra were recorded on a Shimadzu UV-2500 recording spectrophotometer. PL spectra were recorded on a Hitachi F-4500 fluorescence spectrophotometer. Differential scanning calorimetry (DSC) was performed on a NETZSCH DSC 200 PC unit at a heating rate of 10 °C min^{-1} from room temperature to 300 °C under argon. The glass transition temperature (T_g) was determined from the second heating scan. Thermogravimetric analysis (TGA) was undertaken with a NETZSCH STA 449C instrument. The thermal stability of the samples under a nitrogen atmosphere was determined by measuring their weight loss while heating at a rate of 15 °C min^{-1} from 25 to 600 °C. Cyclic voltammetry (CV) was carried out in nitrogen-purged THF (reduction scan) and dichloromethane (oxidation scan), respectively, with a CHI voltammetric analyzer. Tetrabutylammonium hexafluorophosphate ($TBAPF_6$) (0.1 M) was used as the supporting electrolyte. The conventional three-electrode configuration consists of a platinum working electrode, a platinum wire auxiliary electrode, and an Ag wire pseudo-reference electrode with ferrocenium–ferrocene (Fc^+/Fc) as the internal standard. Cyclic voltammograms were obtained at a scan rate of 100 mV s^{-1}. The onset potential was determined from the intersection of two tangents drawn at the rising and background current of the cyclic voltammogram.

2-(4-*tert*-Butylphenyl)-5-(3,5-dibromophenyl)-1,3,4-oxadiazole and 4-(diphenylamino)phenylboronic acid were prepared according to reported procedures.[31]

Synthesis of 2-(3,5-bis(4′-(diphenylamino)phenyl)phenyl)-5-(4-*tert*-butylphenyl)-1,3,4-oxadiazole (TPO). To a mixture of 2-(4-*tert*-butylphenyl)-5-(3,5-dibromophenyl)-1,3,4-oxadiazole (0.872 g, 2.0 mmol), 4-(diphenylamino)phenylboronic acid (1.742 g, 6.0 mmol), $Pd(PPh_3)_4$ (0.092 g, 0.08 mmol), degassed THF (36 ml) and 2 M Na_2CO_3 in distilled water (12 ml, 24.0 mmol) were added. Then the mixture was heated to reflux for 48 h under argon. After cooling to room temperature, the solution was extracted with chloroform and the organic layer was washed with brine and H_2O, then dried over anhydrous Na_2SO_4. After removal of solvent, the residue was purified by chromatography on silica gel (eluent: petroleum/dichloromethane = 1 : 1, v/v). The crude product was recrystallized from ethanol and dichloromethane to afford the compound 0.841 g, yield: 55%. ^{1}H NMR (300 MHz, $CDCl_3$): δ 7.93 (d, J = 8.4 Hz, 2H), 7.50 (d, J = 8.4 Hz, 2H), 7.45 (s, 2H), 7.36 (s, 1H), 7.26–7.21 (m, 14H), 7.10–7.08 (m, 10H), 7.04 (t, J = 7.8 Hz, 4H), 1.34 (s, 9H). ^{13}C NMR (75 MHz, $CDCl_3$): δ 155.61, 148.14, 147.76, 142.43, 133.85, 129.64, 128.24, 127.12, 126.34, 125.18, 124.87, 123.90, 123.56, 123.47, 121.33, 35.37, 31.41. Anal. calcd. for $C_{54}H_{44}N_4O$: C 84.79, H 5.80, N 7.32; Found: C 85.06, H 5.69, N 6.86. MS (ESI): m/z 765 (M^+ + 1).

Computational details

The electronic properties calculation was performed with the Gaussian 03 program package. The calculation was optimized by means of the B3LYP (Becke three parameters hybrid functional with Lee–Yang–Perdew correlation functionals) with the 6-31G (d) atomic basis set. Molecular orbitals were visualized using Gaussview.

Device fabrication and measurement

The devices were fabricated according to the configuration indium tin oxide (ITO)/PEDOT:PSS (80 nm)/emission layer (80 nm)/1,3,5-tris(*N*-phenylbenzimidazol-2-yl)benzene (TPBI, 40 nm)/LiF (1 nm)/Al (100 nm). Commercial ITO coated glass with sheet resistance of 10 Ω $square^{-1}$ was used as the starting substrates. In a general procedure, the ITO glass substrates were pre-cleaned carefully and treated with oxygen plasma for 2 min. Then 80 nm thick PEDOT:PSS film was first spin-coated onto the ITO glass substrates from a water solution and dried at 120 °C for 30 min under vacuum. A mixture of the Ir complexes and the host was later spin-coated from chlorobenzene solution onto the PEDOT:PSS layer and dried at 120 °C for 2 h under vacuum. Then a 40 nm TPBI layer was deposited followed by 1nm LiF as an electron injection layer and the 100 nm thick aluminium layer as the cathode sequentially. The L–V–J of the devices was measured with a Keithley 2400 Source meter and a Keithley 2000 Source multimeter equipped with a calibrated silicon photodiode. The EL spectra were measured using a JY

SPEX CCD3000 spectrometer. All measurements were carried out at room temperature under ambient conditions.

Results and discussion

Synthesis and characterization

The new compound **TPO** was synthesized through the Pd-catalyzed Suzuki cross-coupling reaction of 2-(4-*tert*-butylphenyl)-5-(3,5-dibromophenyl)-1,3,4-oxadiazole and 4-(diphenylamino) phenylboronic acid (Scheme 1). The structure was fully characterized by ^{1}H NMR, ^{13}C NMR, mass spectrometry, and elemental analysis.

The good thermal stability of the compound is indicated by its high decomposition temperature of 457 °C (T_d, corresponding to 5% weight loss) through thermogravimetric analysis (TGA) measurement. The glass transition temperature (T_g) is 131 °C by differential scanning calorimeter (DSC), which is higher than those of the host materials based on triphenylamine/oxadiazole hybrids (92–116 °C) we previously reported.[31] The excellent thermal stability with high T_d and T_g values enables the preparation of homogeneous and stable amorphous thin films through solution processing, which is crucial for the operation of OLEDs.

Photophysical properties

Fig. 1 shows the absorption and photoluminescent (PL) spectra of **TPO**. The absorption around 300 nm could be assigned to a donor-centered π–π* transition, and the longer wavelength ranging from 310 nm to 370 nm could be attributed to a π–π* transition from the electron-rich triphenylamine moiety to the electron-deficient oxadiazole moiety. The PL spectrum of **TPO** in toluene solution exhibits blue emission at 410 nm. The triplet energy (E_T) of **TPO** determined by the highest-energy vibronic sub-band of the phosphorescence spectra at 77 K is 2.44 eV, which suggests that the compound could host green phosphor Ir(ppy)$_3$ (2.42 eV) and orange-red phosphor (PPQ)$_2$Ir(acac) (2.11 eV).

Electrochemical properties and theoretical calculations

The electrochemical properties of **TPO** were probed by cyclic voltammetry (CV), using tetrabutylammonium hexafluorophosphate (TBAPF$_6$) as the supporting electrolyte and ferrocene as the internal standard (Fig. 2). The compound undergoes both reversible oxidation and reduction to permit the formation of stable cation and anion radicals, which implies its bipolar transporting property. During the anodic scan in dichloromethane, a reversible oxidative process occurred at

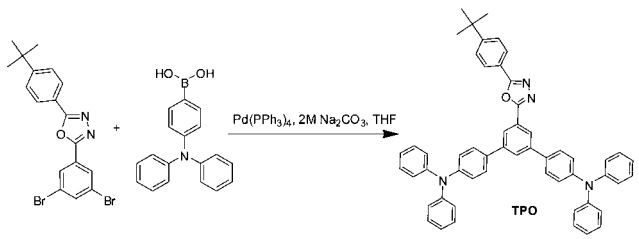

Scheme 1 Synthesis of **TPO**.

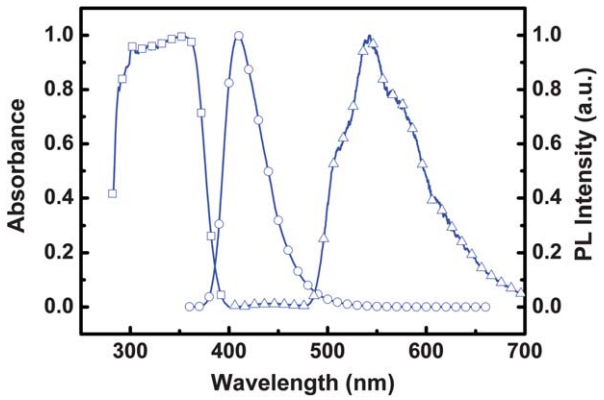

Fig. 1 UV–vis absorption (square) and PL spectra of **TPO** in toluene solution at room temperature (circle), and phosphorescence spectra in film at 77 K (triangle).

0.39 eV, which was derived from the oxidation of triphenylamine units. Upon the cathodic scan in THF, a reversible reductive process at −2.61 eV was detected, which originated from the reduction of the oxadiazole unit. The HOMO and LUMO energy levels are obtained according to the following equations: HOMO = E_{onset}^{ox} (*vs.* Fc$^+$/Fc) + 4.8, LUMO = E_{onset}^{red} (*vs.* Fc$^+$/Fc) + 4.8, respectively. The HOMO level of 5.19 eV is very close to that of PEDOT:PSS (5.20 eV). The LUMO level of 2.19 eV is similar to other oxadiazole derivatives.[31]

The electronic properties of the compound were studied by density functional theory (DFT) calculations using the B3LYP hybrid functional (Fig. 3). The calculated HOMO and LUMO levels are 5.13 and 2.04 eV, respectively, which are in good agreement with the experimental results. According to the DFT calculations, the HOMO orbitals are mainly located on the electron-donating triphenylamine moiety; while the LUMO orbitals delocalize on the electron-accepting oxadiazole moiety. The separation between HOMO and LUMO levels is preferable for efficient hole- and electron-transporting properties and the prevention of reverse energy transfer.[28]

Electrophosphorescent devices

To assess the utility of the compound as a host material for phosphors in solution-processed PhOLEDs, the red-light

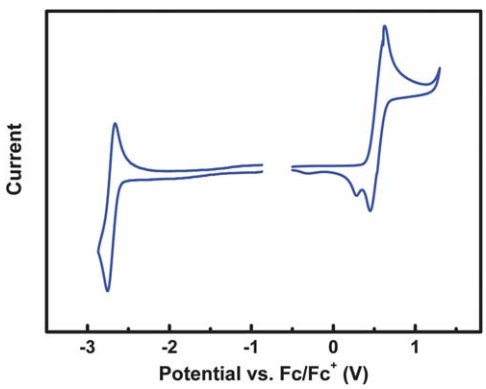

Fig. 2 Cyclic voltammograms of **TPO** in CH_2Cl_2 for oxidation and THF for reduction.

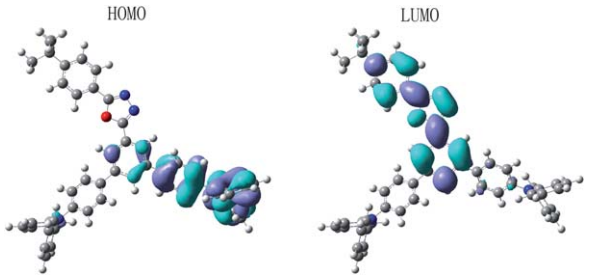

Fig. 3 Spatial distributions of the HOMO and LUMO levels of **TPO**.

emitting device **A** with the configuration: ITO/PEDOT:PSS (80 nm)/**TPO**:5 wt% $(PPQ)_2Ir(acac)$ (80 nm)/TPBI (40 nm)/LiF (1 nm)/Al (100 nm) was firstly fabricated. PEDOT:PSS was used as a smoothing layer for ITO; TPBI acted as electron-transporting and hole-blocking layer; LiF served as electron-injecting layer . The current density–voltage–brightness (*J–V–L*) characteristics and efficiency *versus* current density curves of the device are shown in Fig. 5. EL data are summarized in Table 1. The external quantum efficiency *versus* current density curves of devices are presented in the ESI.†

Device **A** shows red emission around 616 nm with CIE coordinates of (0.64, 0.36) (Fig. 4). The device turns on at a relatively low voltage of 4.9 V for solution-processed PhOLEDs, implying the reduced energy barrier between anode and emission layer due to the high-lying HOMO level of host material. A maximum current efficiency of 13.3 cd A^{-1} and a maximum power efficiency of 8.6 lm W^{-1} were obtained, which are comparable to the best performances of the solution-processed red-light PhOLEDs.[17,32–34] For example, Kim *et al.* reported solution-processed red PhOLEDs with a maximum luminous efficiency of 12.7 cd A^{-1} at CIE coordinates of (0.65, 0.33) using mixed host materials comprised of electron-transporting TPBI and hole-transporting 1,4-bis[(1-naphthylphenyl)amino]biphenyl (NPB);[35] Ding *et al.* presented maximum efficiencies of 13.0 cd A^{-1} and 7.2 lm W^{-1} for red PhOLEDs with a red-emissive dendrimer dispersed in mixed host materials containing electron-transporting 2-*tert*-butylphenyl-5-biphenyl-1,3,4-oxadiazole (PBD) and hole-transporting *N*-(4-[9,3′;6′,9″]tercarbazol-9′-yl)phenylcarbazole (TCCz).[36] We note that the single host **TPO** in this work can function as well as mixed host materials. This reveals its bipolar nature.

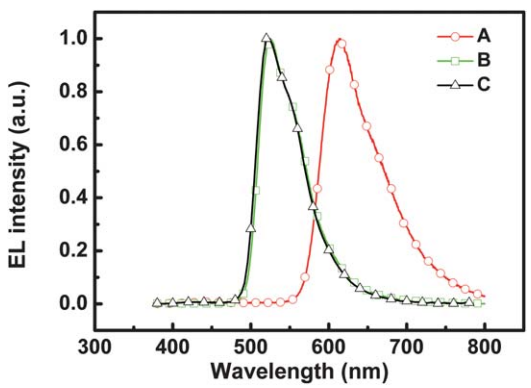

Fig. 4 EL spectra for devices **A–C**.

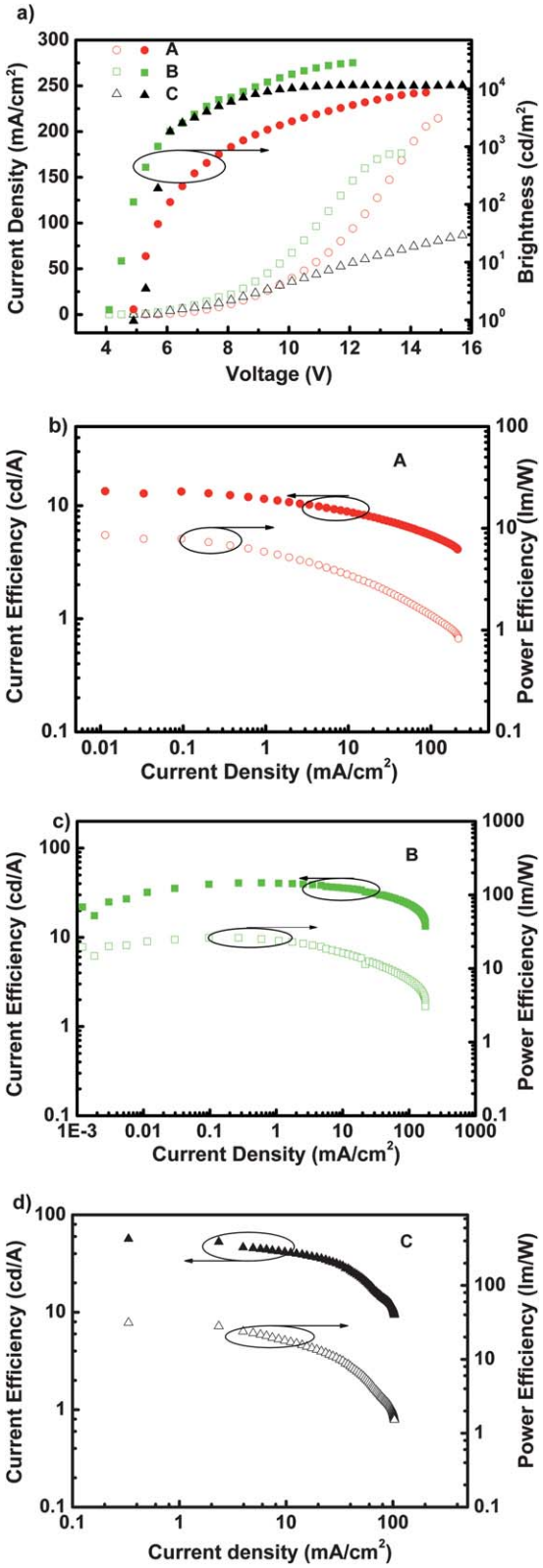

Fig. 5 Current density–voltage–brightness characteristics for devices **A–C** (a); current efficiency and power efficiency *versus* current density curves for device **A** (b), device **B** (c) and device **C** (d).

Table 1 EL data of the devices

Device type	V_{on}[a] (V)	L_{max}[b] (cd m^{-2})	$\eta_{c.max}$[c] (cd A^{-1})	$\eta_{p.max}$[d] (lm W^{-1})	$\eta_{EQE,\ max}$[e] (%)	CIE[f] (x, y)
A	4.9	8680	13.3, 8.7	8.6, 3.4	10.2	0.64, 0.36
B	4.1	28 454	40.8, 39.6	26.3, 21.8	11.0	0.33, 0.63
C	4.9	10 799	56.8, 52.8	31.3, 28.1	15.0	0.32, 0.63

[a] Turn-on voltage. [b] Maximum luminance. [c] Maximum current efficiency, then data at 1000 cd m^{-2}. [d] Maximum power efficiency, then data at 1000 cd m^{-2}. [e] Maximum external quantum efficiency. [f] Measured at 10V.

Subsequently, we fabricated green phosphorescent device **B** by doping **TPO** with 9 wt% Ir(ppy)$_3$ in the same structure as device **A**. Though the triplet energies between host material and guest are close, the EL spectra show typical green emission around 530 nm originating from the guest Ir(ppy)$_3$, suggesting no reverse energy transfer from the guest back to the host. Device **B** shows a maximum luminance of 28 454 cd m^{-2} at 12.3 V, a maximum current efficiency of 40.8 cd A^{-1}, and a maximum power efficiency of 26.3 lm W^{-1}. At a practical luminance of 1000 cd m^{-2}, the efficiencies still remain very high (39.6 cd A^{-1} and 21.8 lm W^{-1}). The very small roll-off can be attributed to the bipolar transport feature of **TPO**. Generally, charge recombination tends to occur close to the interface of the charge-transport layer if the emitting layer lacks the bipolar characteristics. In this work, the less pronounced roll-off value indicates that excitons have been evenly distributed through the emitting layer and that the accumulation of charges and excitons at interfaces has been prevented. The performance of solution-processed **TPO**-hosted green PhOLEDs is competitive with those devices in similar configuration with Ir dendrimers dispersed in small molecules.[37,38]

From the energy level diagram of the device materials (Fig. 6), the electron-injection from the TPBI into EML is energetically unfavorable due to the large barrier between TPBI and **TPO**, therefore we fabricated device **C** using 80 wt% **TPO**:17 wt% PBD:3 wt% Ir(ppy)$_3$ as the EML. PBD was incorporated into the host matrix to facilitate electron-injection and -transporting due to its low-lying LUMO level (2.4 eV) as well as electron-deficient nature. The energy barrier between TPBI and PBD is 0.3 eV, which favors the electron-injection from ETL to EML. Under the same operating voltage, the current density of device **C** is

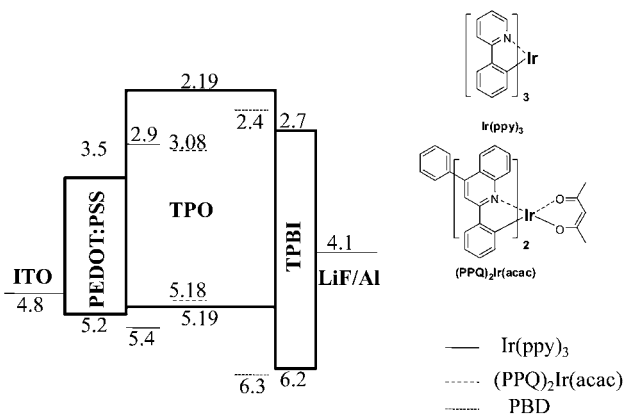

Fig. 6 Proposed energy level diagram of device materials investigated in this work.

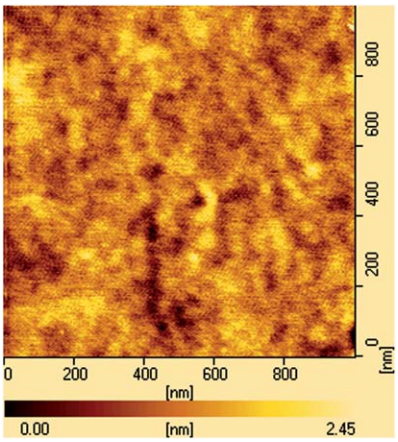

Fig. 7 AFM topographic image of film containing 80 wt% **TPO**, 17 wt% PBD and 3 wt% Ir(ppy)$_3$ after annealing at 120 °C for 1 h under a nitrogen atmosphere.

lower than that of device **B** (Fig. 5a), indicating more balanced and better recombination of carriers. Device **C** exhibits a maximum current efficiency of 56.8 cd A^{-1} and power efficiency of 31.3 lm W^{-1}, which is among the best ever reported for small-molecule based solution-processed green PhOLEDs.[22] Atomic force microscopy (AFM) was used to investigate the morphology of annealed film prepared from **TPO** and PBD blended with 3 wt % Ir(ppy)$_3$ in a 1,2-dichlorobenzene solution onto the PEDOT:PSS layer after annealing at 120 °C for one hour (Fig. 7). The spin-coated film exhibits fairly smooth surface morphology with a small root-mean-square (RMS) surface roughness of 0.34 nm. The results demonstrate that not only the bipolar ability of **TPO** but also the good morphology could contribute to the high efficiencies of solution-processed PhOLEDs.

Conclusions

In conclusion, we have designed and synthesized a bipolar host material **TPO** for solution-processable PhOLEDs. Through *meta*-linkage between the electron-rich and electron-deficient units, favorable localization of HOMO/LUMO levels and proper triplet energy can be realized simultaneously. Highly efficient green and red PhOLEDs through solution processing achieved a maximum current efficiency of 40.8 cd A^{-1} and 13.3 cd A^{-1}, respectively. Moreover, the current efficiency roll-off under high current densities is very small. A further optimized device exhibited a maximum current efficiency of 56.8 cd A^{-1}, which is among the highest ever reported for small-molecule based solution-processed green PhOLEDs.

Acknowledgements

We thank the National Natural Science Foundation of China (Nos. 90922020), the National Basic Research Program of China (973 Program-2009CB623602, 2009CB930603), the Open Research Fund of State Key Laboratory of Polymer Physics and Chemistry, Changchun Institute of Applied Chemistry, Chinese Academy of Sciences, and the Fundamental Research Funds for the Central Universities of China for financial support.

Notes and references

1 M. A. Baldo, D. F. O'Brien, Y. You, A. Shoustikov, S. Sibley, M. E. Thompson and S. R. Forrest, *Nature*, 1998, **395**, 151.
2 L. Xiao, Z. Chen, B. Qu, J. Luo, S. Kong, Q. Gong and J. Kido, *Adv. Mater.*, 2011, **23**, 926.
3 Y. Sun, N. C. Giebink, H. Kanno, B. Ma, M. E. Thompson and S. R. Forrest, *Nature*, 2006, **440**, 908.
4 F. So, B. Krummacher, M. K. Mathai, D. Poplavskyy, S. A. Choulis and V.-E. Choong, *J. Appl. Phys.*, 2007, **102**, 091101.
5 X. Gong, W. Ma, J. C. Ostrowski, G. C. Bazan, D. Moses and A. J. Heeger, *Adv. Mater.*, 2004, **16**, 615.
6 H. Wu, L. Ying, W. Yang and Y. Cao, *Chem. Soc. Rev.*, 2009, **38**, 3391.
7 X. Yang, D. Müller, D. Neher and K. Meerholz, *Adv. Mater.*, 2006, **18**, 948.
8 X. Yang, D. Neher, D. Hertel and T. K. Däubler, *Adv. Mater.*, 2004, **16**, 161.
9 N. Rehmann, D. Hertel, K. Meerholz, H. Becker and S. Heun, *Appl. Phys. Lett.*, 2007, **91**, 103507.
10 H. Wu, G. Zhou, J. Zou, C.-L. Ho, W.-Y. Wong, W. Yang, J. Peng and Y. Cao, *Adv. Mater.*, 2009, **21**, 4181.
11 C. Jiang, W. Yang, J. Peng, S. Xiao and Y. Cao, *Adv. Mater.*, 2004, **16**, 537.
12 Y.-C. Chen, G.-S. Huang, C.-C. Hsiao and S.-A. Chen, *J. Am. Chem. Soc.*, 2006, **128**, 8549.
13 S.-P. Huang, T.-H. Jen, Y.-C. Chen, A.-E. Hsiao, S.-H. Yin, H.-Y. Chen and S.-A. Chen, *J. Am. Chem. Soc.*, 2008, **130**, 4699.
14 X. H. Yang and D. Neher, *Appl. Phys. Lett.*, 2004, **84**, 2476.
15 J. H. Park, C. Yun, T.-W. Koh, Y. Do, S. Yoo and M. H. Lee, *J. Mater. Chem.*, 2011, **21**, 5422.
16 C. H. Chien, S. F. Liao, C. H. Wu, C. F. Shu, S. Y. Chang, Y. Chi, P. T. Chou and C. H. Lai, *Adv. Funct. Mater.*, 2008, **18**, 1430.
17 Z. Ma, J. Ding, B. Zhang, C. Mei, Y. Cheng, Z. Xie, L. Wang, X. Jing and F. Wang, *Adv. Funct. Mater.*, 2010, **20**, 138.
18 K. Zhang, Z. Chen, C. Yang, Y. Tao, Y. Zou, J. Qin and Y. Cao, *J. Mater. Chem.*, 2008, **18**, 291.
19 D. A. Poulsen, B. J. Kim, B. Ma, C. S. Zonte and J. M. J. Fréchet, *Adv. Mater.*, 2010, **22**, 77.
20 X. Gong, H. Benmansour, G. C. Bazan and A. J. Heeger, *J. Phys. Chem. B*, 2006, **110**, 7344.
21 B. Park, Y. H. Huh, H. G. Jeon, C. H. Park, T. K. Kang, B. H. Kim and J. Park, *J. Appl. Phys.*, 2010, **108**, 094506.
22 J.-H. Jou, M.-F. Hsu, W.-B. Wang, C.-L. Chin, Y.-C. Chung, C.-T. Chen, J.-J. Shyue, S.-M. Shen, M.-H. Wu, W.-C. Chang, C.-P. Liu, S.-Z. Chen and H.-Y. Chen, *Chem. Mater.*, 2009, **21**, 2565.
23 L. Duan, L. Hou, T.-W. Lee, J. Qiao, D. Zhang, G. Dong, L. Wang and Y. Qiu, *J. Mater. Chem.*, 2010, **20**, 6392.
24 Z. Q. Gao, M. Luo, X. H. Sun, H. L. Tam, M. S. Wong, B. X. Mi, P. F. Xia, K. W. Cheah and C. H. Chen, *Adv. Mater.*, 2009, **21**, 688.
25 F.-M. Hsu, C.-H. Chien, P.-I. Shih and C.-F. Shu, *Chem. Mater.*, 2009, **21**, 1017.
26 Y. Tao, Q. Wang, C. Yang, Q. Wang, Z. Zhang, T. Zou, J. Qin and D. Ma, *Angew. Chem., Int. Ed.*, 2008, **47**, 8104.
27 Z. Ge, T. Hayakawa, S. Ando, M. Ueda, T. Akiike, H. Miyamoto, T. Kajita and M.-a. Kakimoto, *Chem. Mater.*, 2008, **20**, 2532.
28 Z. Ge, T. Hayakawa, S. Ando, M. Ueda, T. Akiike, H. Miyamoto, T. Kajita and M.-a. Kakimoto, *Adv. Funct. Mater.*, 2008, **18**, 584.
29 Y. Tao, Q. Wang, C. Yang, K. Zhang, Q. Wang, T. Zou, J. Qin and D. Ma, *J. Mater. Chem.*, 2008, **18**, 4091.
30 L. Zeng, T. Y.-H. Lee, P. B. Merkel and S. H. Chen, *J. Mater. Chem.*, 2009, **19**, 8772.
31 Y. Tao, Q. Wang, L. Ao, C. Zhong, J. Qin, C. Yang and D. Ma, *J. Mater. Chem.*, 2010, **20**, 1759.
32 T. D. Anthopoulos, M. J. Frampton, E. B. Namdas, P. L. Burn and I. D. W. Samuel, *Adv. Mater.*, 2004, **16**, 557.
33 S. J. Lee, J. S. Park, M. Song, I. A. Shin, Y. I. Kim, J. W. Lee, J. W. Kang, Y. S. Gal, S. Kang, J. Y. Lee, S. H. Jung, H. S. Kim, M. Y. Chae and S. H. Jin, *Adv. Funct. Mater.*, 2009, **19**, 2205.
34 M. Song, J. S. Park, C.-H. Kim, M. J. Im, J. S. Kim, Y.-S. Gal, J.-W. Kang, J. W. Lee and S.-H. Jin, *Org. Electron.*, 2009, **10**, 1412.
35 H. Kim, Y. Byun, R. R. Das, B.-K. Choi and P.-S. Ahn, *Appl. Phys. Lett.*, 2007, **91**, 093512.
36 J. Ding, J. Lü, Y. Cheng, Z. Xie, L. Wang, X. Jing and F. Wang, *Adv. Funct. Mater.*, 2008, **18**, 2754.
37 S.-C. Lo, N. A. H. Male, J. P. J. Markham, S. W. Magennis, P. L. Burn, O. V. Salata and I. D. W. Samuel, *Adv. Mater.*, 2002, **14**, 975.
38 J. Ding, J. Gao, Y. Cheng, Z. Xie, L. Wang, D. Ma, X. Jing and F. Wang, *Adv. Funct. Mater.*, 2006, **16**, 575.